FOUR-STATION INTERFEROMETRIC RADAR OBSERVATIONS OF MARS EXPLORATION ROVER LANDING SITES.

M. A. Slade[2], K.W. Larsen[1], A. F. Haldemann[2], R.F. Jurgens[2], R. E. Arvidson[1], J.-L. C. Margot[3] ***[1]Dept. Of Earth and Planetary Sciences, Washington University, 1 Brookings Drive, St. Louis, MO 63130, U.S.A; [2]JPL, California Institute of Technology, 4800 Oak Grove Dr. Pasadena CA, 91109,, U.S.A; [3]Geol. & Planet. Sci., Ca1tech, Pasadena, CA, 91125, USA.*** Martin.A.Slade@jpl.nasa.gov , larsen@wundow.wustl.edu , margot@gps.caltech.edu

Abstract. The radar observations carried out on fourteen dates from May 2001 to July 2001 were designed to measure the surface properties of candidate landing sites for the Mars Exploration Rovers. The radar reflectivities and roughness determined at the 3.5-cm radar wavelength are particularly applicable to understanding the landing hazards and the trafficability of the various sites at the size scale that will be experienced by the Rovers. The details of the radar interferometric processing are outlined, since both new hardware and new processing algorithms are being utilized in obtaining and processing of this large data set.

Introduction: During the most recent Mars opposition (centered in July, 2001), fourteen radar observations were made of the planet, as summarized in Table 1, covering Terra Meridiani, Elysium, Isidis Planitia, and Syrtis Major. These regions (Figure 1) were targeted for both their scientific interest as well as their conspicuous applicability to near-future missions. In particular, the Terra Meridiani region, or 'Hematite' region due to the detection of up to fifteen percent crystalline gray hematite on the surface [1], was the target for six of our observations. Also, since the Terra Meridiani region is a leading candidate as a landing site for one of the 2003 Mars Exploration Rovers (MER), radar observations of the region are of a particularly notable nature. This is especially true since radar properties are sensitive to scales on the order of several wavelengths, the same scales as will be experienced by the rovers' motions on the surface.

Date (0 HrUT)	*DIST (AU)*	*Lat (0 Hr UT)*	*Rise Long.*	*Set Long.*
3-May-01	0.6408	-1.825	320.9	35.2
5-May-01	0.6270	-1.819	301.4	15.7
17-May-01	0.5530	-1.277	200.5	252.8
19-May-01	0.5423	-1.099	181.1	233.5
28-May-01	0.5006	0.002	92.8	141.6
7-Jun-01	0.4684	1.696	354.1	39.2
8-Jun-01	0.4660	1.884	345.2	29.1
9-Jun-01	0.4638	2.074	335.2	19.1
17-Jun-01	0.4522	3.625	257.0	297.3
22-Jun-01	0.4502	4.561	205.6	245.8
1-Jul-01	0.4564	5.999	115.9	154.9
2-Jul-01	0.4578	6.131	105.8	144.8
14-Jul-01	0.4844	7.181	345.9	23.7
23-Jul-01	0.5143	7.275	254.2	292.0

Table 1: Parameters for the fourteen observations of Mars during the 2001 opposition.

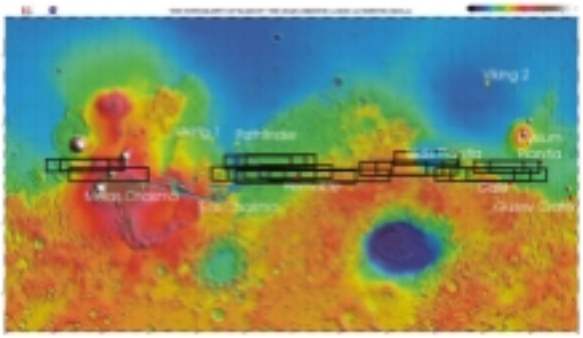

Figure 1: Extent of opposition observations overlain on MOLA topography.

Observations: A PN range-coded X-band (3.5-cm) radar signal was transmitted by the 70-meter telescope at the Goldstone Deep Space Communications Complex (GDSCC) and the reflected signal was, for the first time, recorded simultaneously at four GDSCC telescopes. Previous interferometric observations of Mars and Venus have used up to three telescopes [2]. The increase to four telescopes doubles the number of interferometric baselines from 3 to 6, thus improving the input for the statistical method used in interferometric processing, further described below. However, in summary, the third and fourth stations are needed to add additional baselines instantaneously so that we need not rely on Earth rotation to provide projections of the baselines over long integration times to sample the radar brightness distribution. Thus we can reduce the Doppler smearing to the minimum supported by the experiment's signal-to-noise (SNR).

Also new this opposition was the use of the Portable Fast Sampler (PFS) data recording system [3]. Each telescope has a dedicated PFS data acquisition system that records the I and Q channels of the "expected" (opposite circular from transmitted or OC) polarization at four megahertz and with four bits per channel. Over the course of the fourteen observations, this yielded a total data volume in excess of one terabyte..

There are two major advantages to the PFS system for Mars interferometry: Firstly, the use of the PFS's removes the necessity of trying to range-align all four stations in real time. Secondly, prior to the introduction of the PFS system, powers and cross-powers between the telescopes were computed by hardware and only the product recorded. The PFS boxes record the raw data stream, relying on post-processing to calculate the needed powers and cross-powers. Thus, summing periods (both coherent and incoherent sums) can be chosen at will. Using shorter incoherent summing periods is integral to reducing the amount of down-track smearing.

Processing: Processing of the collected data is a multi-step process. The first main step of the processing does range alignment, baud integration of the code symbols, and demodulation of the range code. At this point, we have a series of range-gated signals that are Fast-Fourier transformed to create a complex delay-Doppler frame (also know as a "single look" frame). Averaging looks provides a delay-Doppler image, of which a typical example is shown in Figure 2. (The single look frames can be averaged until either the phase drift or the planet rotation causes smearing of the images.) The next processing step forms the power and cross-power pairs from the (complex) single looks.

Next the data from each station is processed individually to produce a profile of the sub-radar track. Along this profile, the data from the leading edge of the reflected signal is fit to the Hagfors model [3]. Fitting this data to the Hagfors model, and also extracting the range information, yields information about the surface properties within the resolution cell. Since there is no interferometric processing done at this stage, the resolution cell is ambiguous in its north-south direction. The resolution cells for these observations are approximately 4 kilometers east-west and 133 kilometers north-south.

Finally, simultaneous maps of reflectivity and altimetry are constructed for each day by use of the Maximum Lik e-lihood Function Method, as described in more detail below.

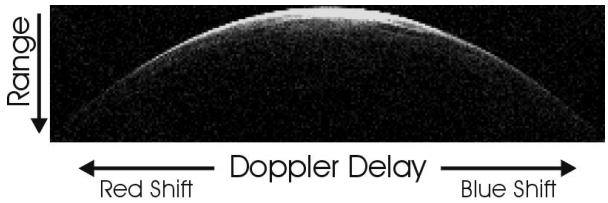

Figure 2: A typical range/delay-Doppler image from the May 3, 2001 of Terra Meridiani. The central longitude is approximately 4.5° W, and central latitude is 1.8° S. The total frequency coverage is ~4 kHz.

With the increased variety and extent of available data sets since the Mars Global Surveyor mission, the comparison and fusion of disparate data sets has become an immensely valuable and scientifically lucrative endeavor. In that vein we have compared the results of the radar profiling to a number of global data sets. Specifically, we have correlated features seen in the profiles of dielectric constant and surface roughness with the region of high hematite content, between 0° and 8° West longitude. This enhancement in the dielectric constant can be modeled with the loaded dielectric model, and is consistent with the measured fifteen percent hematite content [1].

Details of Current Work: Phase 1 of this project entails the profile processing of all the data collected during the 2001 opposition. Included in this phase is the preparation and release of the calibrated data to the Planetary Data System. All the necessary documentation and supporting data is currently being collated, with an anticipated release date of Summer 2002 to the PDS node.

The second phase of the project will focus on the processing of the four-station interferometry. This will culminate in the creation of 3-d radar images of the regions shown in Figure 1. We will use the Maximum Likelihood Function

Method (MLFM), a statistical formulation that solves for the surface reflectivity (or backscatter coefficient) while taking into account a random Gaussian noise component [5]. The resulting data matrices can then be fit to the Hagfors' model, creating 2-d maps of surface roughness and dielectric constant. They also result in an image of the altimetry of the region. These map products will then allow further comparison to global surface properties in an attempt to better understand the surface at radar scales.

More details of the MLFM are provided to give some insight into the theory and the data processing operations of multi-station interferometry. The fundamental concepts of the derivation of altimetry by use of delay-Doppler interferometry have been given by [6] and [7]. The three-station interferometer is a simple extension of the basic two-station interferometer as presented there and the signal processing concepts given by [8]. We begin by considering the two-station, or bistatic, interferometer and its weakness in determining the altimetry. The voltage equations that follow are presented in a phase-normalized manner; i.e., the first station is chosen as a zero-phase reference. In practice, this condition is established by comparing the phase of a large number of points on the planet located along regions having a fringe phase equal to $\pm n\pi$. This procedure has been described in [8].

Equations (la) and (1b) represent electrical voltages received by two antennas in the interferometer. The voltages V_N and V_S represent the signals received from the delay-Doppler resolved regions in the northem and southern hemispheres and are considered to be composed of the vector sum of the signals scattered from a very large number of independent reflectors within the resolved regions; hence they are samples of a complex Gaussian random process; h_N and h_S are the heights of the two regions measured normal from the apparent Doppler equator:

$$V_1 = V_N + V_S + n_1 \tag{1a}$$

$$V_2 = V_N e^{juh_N} + V_S e^{juh_S} + n_2 \tag{1b}$$

The spatial fringe frequency in radians per unit length, u, is dependent upon the locations of the stations and the geometry of the Earth-Mars system. The n_K are additive noise which are independent for each station. In general, we would like to determine V_N and V_S or their powers, and h_N and h_S . Since V_1, V_2, V_N, and V_S are complex, there are six unknowns and only four equations. Therefore no general solution is possible. During the day, however, a large number of such equation sets can be measured, but since V_N and V_S are independent random realizations, there always remain 2n + 2 unknowns and 2n equations, where n is the number of complex equation pairs. Therefore we endeavor to find a statistical solution that best represents the measured voltages. Since V_N and V_S are viewed as zero mean Gaussian random variables, expectations .of their magnitudes squared are nonzero and are proportional to the backscattered powers P_N and P_S from each region and are usually called reflectivities when properly scaled. Unfortunately, in the simple case when u is constant, the resulting statistical equations reduce to a set that is not adequate for the simultaneous solution of P_N, P_S, h_N, and h_S in all regions of the image. The number of unknowns may be reduced by setting h_N and h_S to the values for a perfectly spherical planet, and P_N and P_S may be estimated by a range of suboptimum to optimum procedures. Fortunately, u varies adequately during the day if the observing period includes times near rise and set of the planet, and a solution for all four parameters may be possible. The strength of the solution is strongly dependent upon the amount of variation in u and upon the approximate phase angle uh associated with each delay-Doppler cell. The estimations are further complicated by additive noise from the receiver system, the sky background, and the thermal radiation from Mars itself. In fact, the noise component is often larger than the signal component, tending to obscure the small phase variations caused by departures of h_N and h_S from the perfect sphere. In light of these difficulties the two-station altimetry maps remain an impressive demonstration of the statistical method.

The three-station interferometer gains its power by adding a third complex equation as shown in the following phase-normalized equations:

$$V_1 = V_N + V_S + n_1 \tag{2a}$$

$$V_2 = V_N e^{juh_N} + V_S e^{juh_S} + n_2 \tag{2b}$$

$$V_3 = V_N e^{jvh_N} + V_S e^{jvh_S} + n_3 \tag{3c}$$

As before, there are six unknowns, but there are now six equations (conceptually, ignoring the small noise) providing some hope for a solution. In fact, since V_N and V_S are random, there are certain realizations for which no solution is possible, the simplest being the cases where V_N, V_S, or both are zero. If, however, the equation set is not otherwise ill-conditioned, one or more solutions for V_N, V_S, h_N, and h_S can be found. Simple averages of $|V_N|^2$ and $|V_S|^2$ give estimates of P_N and P_S, while h_N and h_S are determined uniquely for each realization, i.e., there is no speckle noise associated with the altimetry as there is with the reflectivity. The addition of noise to the three-station equations necessitates a statistical

solution unless the signal to noise ratio is sufficiently large that the noise can be viewed as a small perturbation in the equations. Generally, this is not the case. A number of suboptimum estimators have been tried, but a full maximum likelihood estimator has given the best results obtained so far. By this technique, the model parameters P_N, P_S, h_N, and h_S are systematically adjusted to maximize the probability of having received the entire data set associated with each north and south delay-Doppler pair. The generalization to M-station interferometry is straightforward, and basically just increases the robustness of the solution by adding more baselines, and decreases the necessity for data near Mars rise/set.

For the 2001 Mars observations, we note that the entire data set for a single day's operation consists of ~150,000 delay-Doppler frames. Each delay-Doppler frame consists of 64 range-gated spectra having 256 complex points per spectrum, for each of the four stations.

At the present resolution, cross spectra formed between the station pairs may be averaged for the period of 15 seconds without causing appreciable smearing of the maps. This provides about a 200 to 1 data reduction. Further averaging is generally not possible owing to the rotation of the planet, the gradual shift of the apparent equator, and the variation in the interferometric fringe frequencies u, v, w, etc. with time. The maximization of the likelihood function has been carried out by differentiating the likelihood function with respect to P_N and P_S and setting the resulting equation pairs to zero. This yields a nonlinear cross-coupled equation pair in the variables P_N and P_S that can be solved by iteration if h_N and h_S are held constant. The solution is obtained by a simple gradient procedure while holding P_N and P_S constant. The gradient procedure requires the evaluation of both first and all second partial derivatives of the likelihood function with respect to h_N and h_S. Analytic expressions for these have been formed in order to avoid difficulties with numeric differentiation. The reflectivity and altimetry solutions are alternately iterated until adequate convergence is indicated or divergence occurs. Divergence problems are handled in a wide variety of ways depending upon the nature of the problem.

The MLFM processing presumes that, for each pixel in the time series, a Hermetian matrix of power and cross power values can be formed. Each look generates these matrices. However, the origin of these looks track through delay-Doppler space as the planet rotates. A series of such matrices provides a statistical sampling that can be used to estimate the signal power from each hemisphere and the altitudes from which it arises. In general, the unknown parameters are adjusted to give the best statistical match to the data. The starting point for the topography solution will be the MOLA data for the relevant area, which should speed the convergence of the solution greatly and actually gives us a way to calibrate the relative phases between all the antennas. Since the topography is known rather well, the actual ray paths to each pixel is known. Since the topography in view is ever changing, this process has to be done in a continuous manner. Phase drifts are caused by variations in the atmosphere, ionosphere, temperature changes in the antenna and receiver systems, and unmodeled motions of the antenna during tracking.

References:

[1] Christensen, P. R., J. L. Bandfield, R. N. Clark, K. S. Edgett, V. E. Hamilton, T. Hoefen, H. H. Kieffer, R. O. Kuzmin, M. D. Lane, M. C. Malin, R. V. Morris, J. C. Pearl, R. Pearson, T. L. Roush, S. W. Ruff, and M. D. Smith,, "Detection of crystalline hematite mineralization on Mars by the Thermal Emission Spectrometer: evidence for near-surface water," *Jour. Geophys. Res.*, 105, No. E4, 9623-9642, 2000.

[2] Jurgens, R.F., R. M. Goldstein, H. Rumsey, and R. R. Green, "Images of Venus by Three-Station Interferometry - 1977 results," *Jour. Geophys. Res.*, 85, 8282-8294, 1980.

[3] Margot, J.-L."A low-cost portable fast sampling system for astronomical applications," this meeting, 2002.

[4] Hagfors, T., "Backscattering from an undulating surface with applications to radar returns from the Moon," *Jour. Geophys. Res.*, 69, 3779-3784, 1964.

[5] Larsen, K. W., A. F. Haldemann, R.F. Jurgens, R. E. Arvidson, and M. A. Slade., "New Radar Observations of Terra Meridiani," *Eos. Trans. AGU, 82*, No.47, Fall Meeting Supplement, Abstract P42A-0559, 2001.

[6] Zisk, S. H., Lunar topography: First radar-interferometer measurements of Alphonsus-Ptolemaeus-Arzachel region, *Science*, 178, 977-980, 1972.

[7] Shapiro, I. I., S. H. Zisk, A. E. E. Rogers, M. A. Slade, and T. W. Thompson, Lunar topography: Global determination by radar, *Science*, 178, 939-948, 1972.

[8] Rumsey, H. C., G. A. Morris, R. R., Green, and R. R. Goldstein, A radar brightness and altitude image of a portion of Venus, *Icarus*, 23, 1-7, 1974.

Acknowledgements. JPL, a division of the California Institute of Technology, supported this work by grants from NASA's Office of Space Science, Washington, D.C. K. Larsen and R. Arvidson were supported in part by the NASA Planetary Geology and Geophysics Program through Grant NAG5-7830 from the Goddard Space Flight Center. Jean-Luc Margot is an O.K. Earl Postdoctoral Fellow at the California Institute of Technology.